SMAR 2019 – Fifth Conference on Smart Monitoring,
Assessment and Rehabilitation of Civil Structures

SMAR 2019

Local and global state parameter extraction from ambient vibration measurements on bridges

Philipp KÄHLER [1], Yuri PETRYNA [1]
[1] Technische Universität Berlin, Berlin, Germany

Contact e-mail: philipp.kaehler@tu-berlin.de

ABSTRACT: Structural health monitoring of bridges is a topic of research and development since long. Impressive progress has been achieved in the last decades, especially due to a rapid development of measurement and communication techniques as well as that of new theoretical methods. Some tasks like operational modal analysis (OMA) can already be solved very efficiently and reliably. Some others like local damage detection and localization are still a challenge both for research and application.

The present contribution is dedicated to some new techniques for structural health monitoring and its application to bridges. One method under consideration is based on the Hilbert-Huang Transform (HHT) which exhibits a good potential for the extraction of state parameters from vibration measurements under operation conditions. For example, the vibration decay after a truck passage can be used to extract important information on the bridge condition. The Hilbert transform combined with the Empirical Mode Decomposition by Huang allows the identification of the instantaneous vibration frequencies, phases and damping ratios for individual vibrations modes as well as their nonlinear changes due to the vibration amplitude and damage. The damping and nonlinear effects are known to be more sensitive to local damage than the fundamental frequencies. The monitoring of the same short-term parameters after each truck passage enables to develop a long-term monitoring strategy by use of regular time intervals in hours, days, weeks, months and years. By variation of the sensor location it is also possible to localize damage by use of HHT.

This contribution shows the application of the presented monitoring technique to a road bridge and a foot bridge in Berlin.

1 HILBERT-HUANG-TRANSFORM

The HHT is a method which is able to analyze a nonlinear or non-stationary signal by decomposing the signal with the help of the empirical mode decomposition (EMD) in so called intrinsic mode functions (IMF) followed by the application of the Hilbert Transform (HT) on those received IMFs.

On the following pages, both the theoretical background as well as two practical examples for the HHT will be displayed. At first the Hilbert transform and the extracted information from that will be explained and illustrated with a constructed example. After that the empirical mode decomposition and its use is demonstrated with real measurement data from a road bridge in Berlin. Finally, the detection of change in state parameters on a foot bridge in Berlin will be visualized.

1.1 Hilbert transform

The Hilbert transform H of a signal $x(t)$ is a linear operator which is given by convolution of $x(t)$ with the function $1/(\pi t)$ as shown in Eq. 1

$$H\big(x(t)\big) = \frac{1}{\pi} \cdot \int_{-\infty}^{\infty} \frac{x(t)}{t-\tau} \mathrm{d}\tau \quad . \tag{1}$$

If $x(t)$ is a real valued signal, the HT of $x(t)$ results in the same real valued signal, whose phase is shifted by $\pi/2$ while its amplitudes are kept at the same level as before.

This is used to create a complex valued analytical signal $a(t)$, in which the real part of the complex signal is the original signal $x(t)$ and its imaginary part is the HT of $x(t)$ as shown in Eq. 2

$$a(t) = x(t) + i \cdot H\big(x(t)\big) \quad . \tag{2}$$

As a result it can be said, that as long as the HT of $x(t)$ exists, an analytical signal $a(t)$ can be created out of $x(t)$. Analytical signals are well known and widely used in signal processing because they have special properties, which can be seen in Feldman (2011).

Let $x(t)$ be a real valued decaying signal of a system with just one natural frequency. This signal is described by the following properties:

$$x(t) = \begin{cases} 2 \cdot e^{(-0{,}47 \cdot t)} \cdot \sin(2\pi f_1 t) & 0\mathrm{s} \le t < 4\mathrm{s} \quad f_1 = 10\ \mathrm{Hz} \\ 0{,}72 \cdot e^{(-0{,}97 \cdot t)} \cdot \sin(2\pi f_2 t) & 4\mathrm{s} \le t \le 8\mathrm{s} \quad f_2 = 10{,}3\ \mathrm{Hz} \end{cases} \quad . \tag{3}$$

At time $t = 4\mathrm{s}$, there is a new impact on the system resulting in a step in the amplitudes and a slight change in the natural frequency from $f_1 = 10$ Hz to $f_2 = 10{,}3$ Hz. After applying the HT on this non-stationary signal $x(t)$, the associated analytical signal $a(t)$ can be calculated and is depicted in Fig. 1.

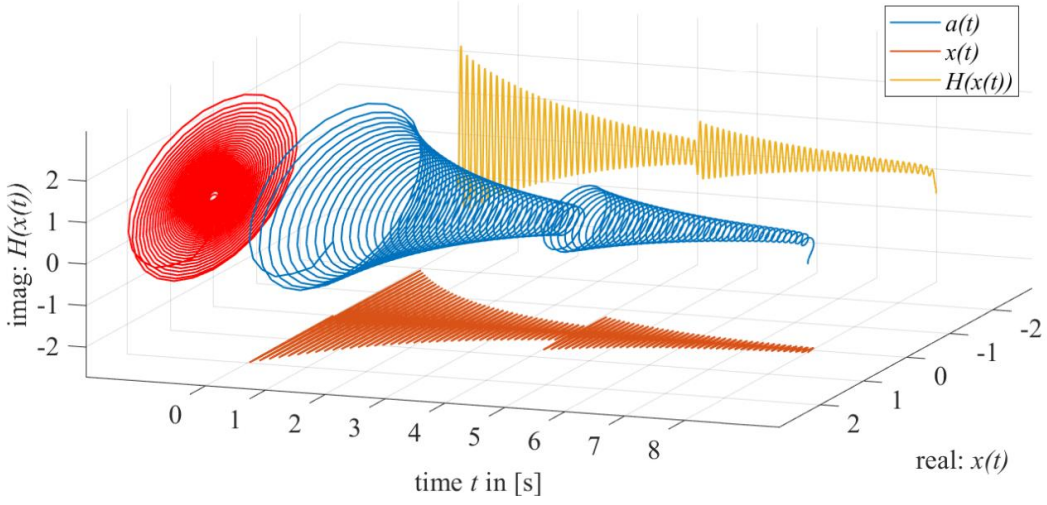

Figure 1. Analytical signal $a(t) = x(t) + i \cdot H\big(x(t)\big)$.

Due to the phase shift of π/2 the imaginary part of $a(t)$ lags behind its real part, which leads to the shown 3D spiral plot. More properties of the analytical signal can be extracted, while taking a closer look at the real-imaginary plane of $a(t)$ shown in Fig. 2.

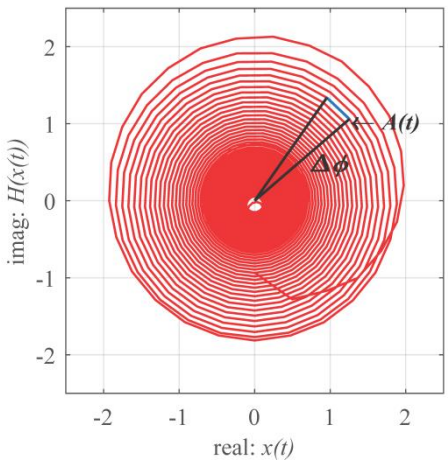

Figure 2. Analytical signal in the real-imaginary plane.

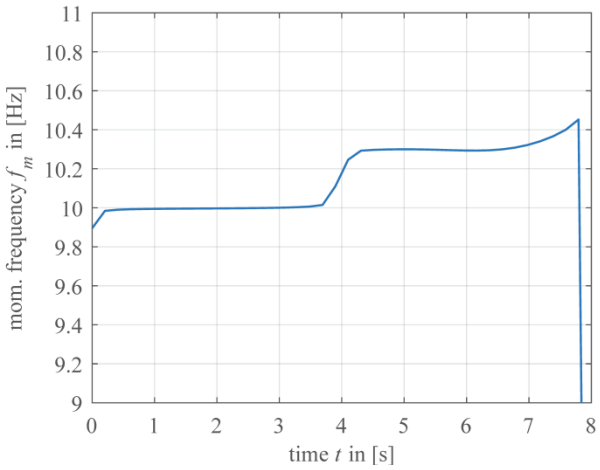

Figure 3. Instantaneous vibration frequency.

Every point of the complex function $a(t)$ at time step t can be described by the instantaneous amplitude A(t) and its instantaneous phase $\phi(t)$. Determining the numerical derivative of $\phi(t)$ with respect to t yields the instantaneous frequency $f_m(t)$ which is shown in Eq.4 and visualized in Fig. 3.

$$f_m(t) = \frac{1}{2\pi} \cdot \frac{\Delta\phi}{\Delta t} \tag{4}$$

Not only the change in frequency at time $t = 4$ s can be clearly observed but also the resolution in time- and frequency-domain is very high due to the fact that $a(t)$ contains information of the phase at every time step t. This makes the HT a valid alternative to the short-time Fourier transform (STFT). The only problems are the edges of the signal where the HT cannot approximate the correct values of $x(t)$. This leads to incorrect instantaneous frequencies in those areas, see Feldman (2011).

1.2 Empirical mode decomposition

In general, ambient vibration measurement signals of bridges contain responses of more than just one natural frequency of the bridge. Therefore, these signals need to be decomposed in signal parts $y_i(t)$, which consist of only one frequency component. The resulting intrinsic mode functions (IMF) are suitable for the HT to be applied on. The method used for the decomposing of the original signal is the empirical mode decomposition (EMD).

In the following, the EMD will be explained step by step. Let $x(t)$ be a real valued signal consisting of more than one natural frequency.

1. Determine the local extreme values of $x(t)$.
2. Construct an upper envelope function through the local maxima $e_+(t)$ and a lower envelope function through the local minima $e_-(t)$ with the help of cubic splines.
3. Calculate the local mean $m(t)$ at every time step t.

$$m(t) = \frac{e_+(t) + e_-(t)}{2} \tag{5}$$

4. Extract a preliminary IMF $z_j(t)$.

$$z_j(t) = x(t) - m(t) \tag{6}$$

5. Check, whether $z_j(t)$ is a stable IMF with just one frequency component. If that is not the case, repeat steps 1-5.
6. If $z_j(t)$ is a stable IMF, save it.

$$y_i(t) = z_j(t) \tag{7}$$

7. Subtract the found IMF $y_i(t)$ from the original signal $x(t)$ to get a residual.

$$res(t) = x(t) - y_i(t) \tag{8}$$

8. Set the residual $res(t)$ as the next $x(t)$ and repeat steps 1-7 on the residual until no more IMF exists, see Gonzales et al. (2014), Zeiler (2012).

For better understanding, the application of the EMD is shown on real measurement data from a road bridge. This bridge is called Sieversbrücke, a reinforced pre-stressed concrete bridge with a length of 77,5 meters which spans over the Teltow Kanal in Berlin, as seen in Fig. 4 and 5. It has a gap in the middle which results in the independence of both roadways.

Figure 4. Side view of the Sieversbrücke.

Figure 5. Bottom view of the Sieversbrücke with cables and the gap between both roadways.

The data was recorded with 3D geophones at the top of one of the roadways of the bride during a 30-minute session. For the demonstration of the EMD just one decaying signal of one of those geophones will be used.

The results of the EMD can be seen in Fig. 6. At first, the IMF 1 is extracted out of the original signal $x(t)$. After that, the IMF will be subtracted from $x(t)$. The residual after the first IMF now contains one frequency component less and it is chosen as the new starting point for the iterative algorithm of the EMD. It should be noted that the IMFs are extracted in order from the highest frequency to the lowest.

The algorithm of the EMD is easy to understand but contains some major difficulties e.g. mode-mixing, envelope creation, and edge problems of the signal, as described in Deering et al. (2005), Fosso et al. (2017), Rilling et al. (2006), Zeiler (2012).

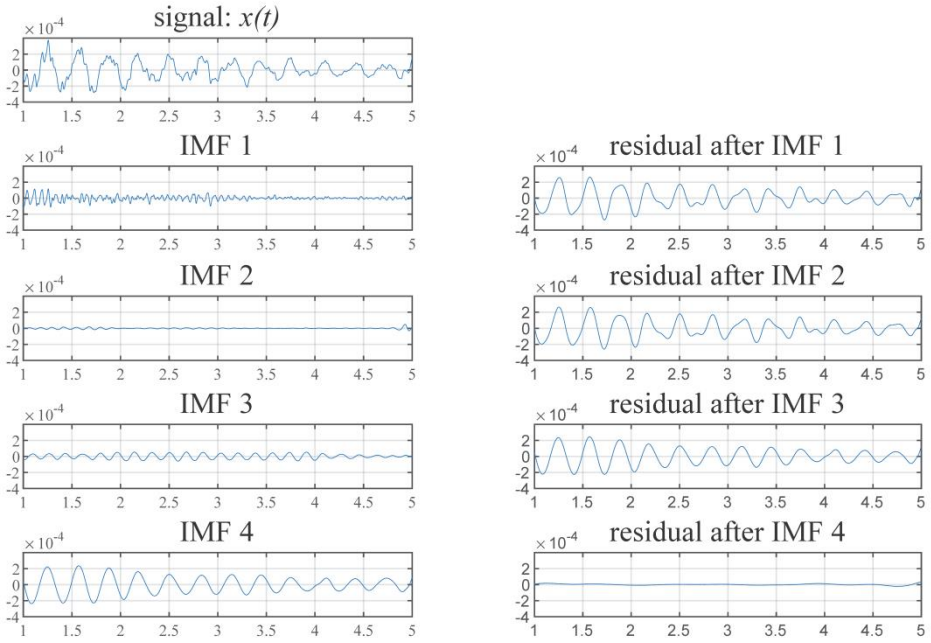

Figure 6. EMD of a decaying signal from the Sieversbrücke.

2 STATE PARAMETERS FOR SHM

After extracting the IMFs from the signal there are mainly two global state parameters which can be determined. First, the application of the HT on the IMFs yields the instantaneous vibration frequencies of each IMF. These instantaneous frequencies correspond to the natural frequencies of the system as long as there are no periodic loads applied on the system. In Fig. 7, it can be seen that the natural frequencies of the bridge which were determined with classic OMA methods (Brincker et al. (2000)) overlay with the instantaneous vibration frequencies from the HHT for the first two modes.

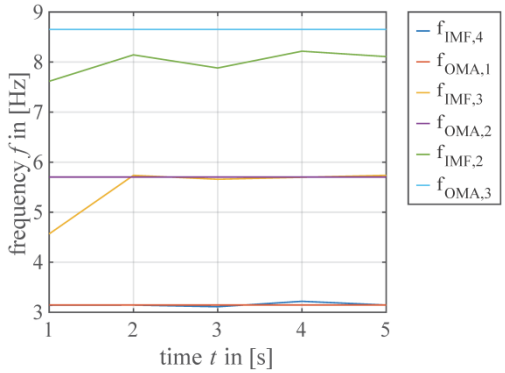

Figure 7. Comparison of natural frequencies from OMA with instantaneous vibration frequencies from HHT.

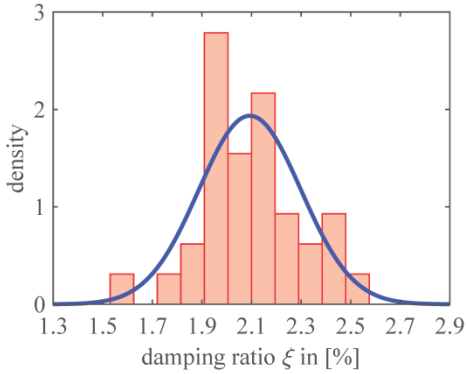

Figure 8. Modal damping ratio of the first bending mode from the Sieversbrücke.

Only the third frequency component shows larger differences. This frequency corresponds to the IMF 2 which has not been stimulated by the ambient load as seen in Fig. 6. Consequently, if an IMF is extracted from the signal while its corresponding natural frequency is not stimulated by the load the HHT can lead to false identified natural frequencies.

Thus, the first state parameter which can be monitored with the help of HHT is the possible change of the natural frequencies over time if these frequency components are stimulated by the load.

The second state parameter is the modal damping ratio. If the measured signal is a decaying signal as in Fig. 6 the IMFs show the vibration decay of the system for each natural frequency, individually. With the help of classic OMA methods like the Frequency Domain Decomposition (FDD) the corresponding natural modes can be determined. In conclusion, the modal damping ratio for each natural mode can be extracted from the IMFs with the logarithmic decrement as long as those IMFs have the characteristic decaying behavior from the original signal.

The modal damping ratio for the first bending mode of the Sieversbrücke is depicted in Fig. 8. It was extracted out of 35 IMFs with the corresponding natural frequency of $f_1 = 3{,}13$ Hz. The results were fitted by a Gaussian distribution which leads to a mean value for the damping ratio of $\xi_{mean} = 2{,}09$ %. In comparison, the damping ratio for the first bending mode determined by the FDD has exactly the same value.

An advantage of the modal damping ratio in comparison to the natural frequency is its sensitivity to a local change in the system which will be shown in the next example. Moreover, with the HHT the modal damping ratio can be determined with respect to time and amplitude of the signal which can lead to the discovery of nonlinearities.

Local state parameters can be extracted by pointwise strain-measurements, which will not be a topic in this paper.

3 PRACTICAL EXAMPLE: VOLKSPARKSTEG

The object of interest is a cable-supported steel bridge with a length of 68,7 meters. This foot bridge is called Volksparksteg and it is located in Berlin, Wilmersdorf. It consists of two longitudinal hollow rectangle beams which are connected by crossbeams. The bridge is supported by a pylon and supports at both ends, as shown in Fig. 9 and 10.

Again, the data was recorded with ten 3D geophones during a three-hour session. Different load scenarios were tested but in this paper only the signals after single impact loads will be discussed due to the decaying characteristic of those occurring signals.

Figure 9. Volksparksteg.

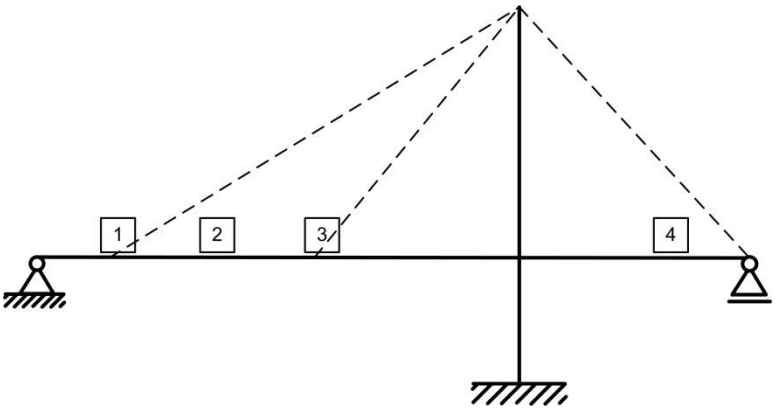

Figure 10. Static system of the Volksparksteg.

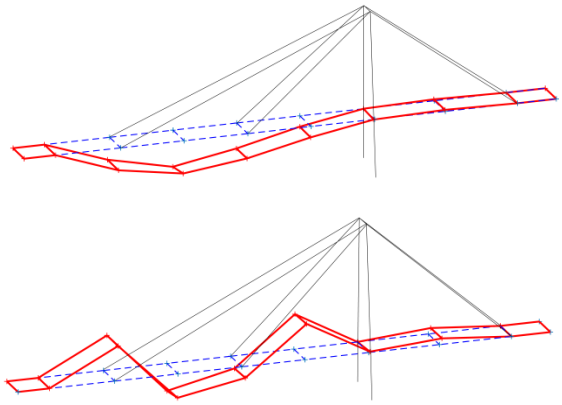

Figure 11. First and third bending mode at $f_1 = 2{,}15$ Hz and $f_2 = 8{,}50$ Hz determined by FDD.

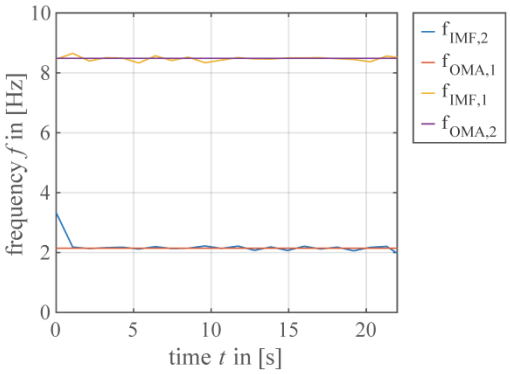

Figure 12. Instantaneous frequencies determined by HHT.

First, single impact loads at points 1, 2, and 3 (see Fig. 10) were used for the determination of the stimulated natural modes and frequencies with the FDD (see Fig. 11). Thereafter, the HHT was used on the same signals to calculate the instantaneous frequencies which are shown in Fig. 12. Both, the FDD and the HHT deliver the same results in regard to the natural frequencies. It should be noted, that the amplitudes of the third bending mode at $f_2 = 8{,}50$ Hz lie within the range of measurement noise. As a result of that, the damping ratio can only be determined for the first bending mode.

Another goal of this algorithm is to detect changes in the state parameters. Therefore, an extra mass $m \cong 1 \ldots 1{,}5$ t has been applied on different spots of the bridge to see if the natural frequencies and modal damping ratios are sensitive to this change. This mass will lead to pre-deformations, other stress levels in the cables and thus to a change in the system.

In the first load scenario the extra mass is put on point 2 (see Fig. 10). At this location the mass influences the first and third bending mode directly. The results of the natural frequencies and the modal damping ratio of the first bending mode are shown in Fig. 13 and Fig. 14. Both, the frequencies and the damping ratio changed after applying the mass. Moreover, the second natural frequency scatters around the correct value. An explanation for this could be that the mass pushes the system into the first bending mode already. Thus, the third mode is not activated properly, which is why this frequency cannot be extracted perfectly.

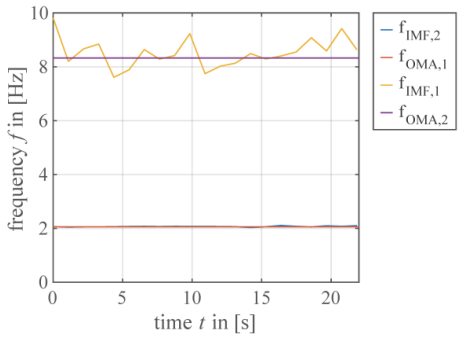

Figure 13. Instantaneous frequencies $f_1 = 2{,}06$ Hz and $f_2 = 8{,}32$ Hz.

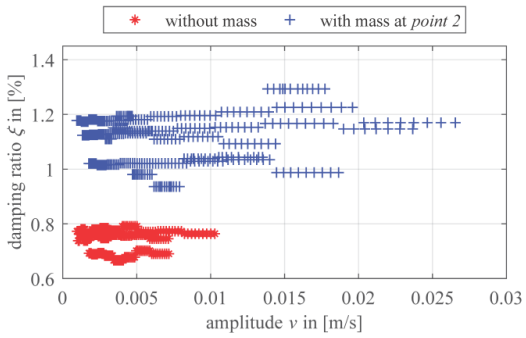

Figure 14. Modal damping ratio for the first bending mode with mass at point 2 and without mass.

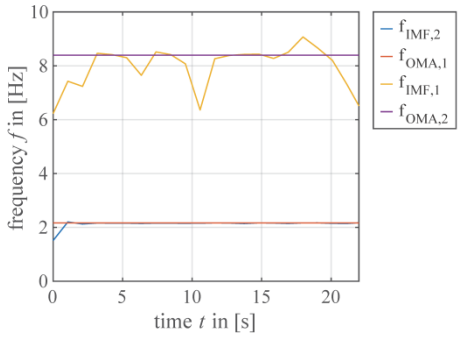

Figure 15. Instantaneous frequencies $f_1 = 2{,}15$ Hz and $f_2 = 8{,}42$ Hz.

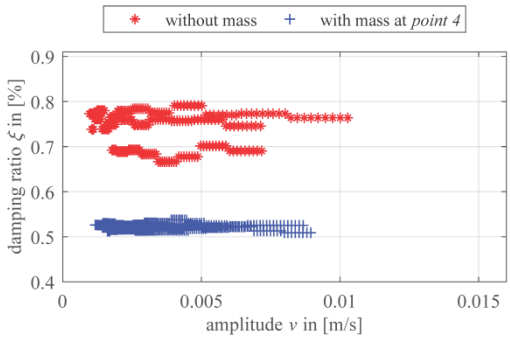

Figure 16. Modal damping ratio for the first bending mode with mass at point 4 and without mass.

In the second load case the extra mass is applied on point 4 (see Fig. 10). This will not influence the first and third bending mode directly since the amplitudes of motion of point 4 are very small in those modes (see Fig. 11). Nevertheless, a change in the damping ratio of the first bending mode can be observed as shown in Fig. 16 even though this change has not been in the same spot than the measurement sensors. Although there is a change in the damping ratio, the natural frequencies stay at the same level.

This leads to the assumption that the modal damping ratio is more sensitive to a change in the system than the natural frequencies.

4 CONCLUSIONS

In this paper, the theoretical background of the HHT has been explained and its application has been illustrated on two practical examples. The HHT yields instantaneous frequencies and modal damping ratios with respect to time or amplitude which are more sensitive to changes in the system than the averaged modal properties extracted by the methods of OMA. Furthermore, a system change in the foot bridge as a consequence of the extra mass could be detected.

Thus, the HHT has great potential in the detection of system change. Moreover, it provides new possibilities for a permanent structure health monitoring system due to the fact that just a few sensors are needed to provide good data.

5 REFERENCES

Brincker, R., L. Zhang, and P. Andersen, 2000, Modal Identification from Ambient Responses using Frequency Domain Decomposition., *Proceedings of the 18th international modal analysis conference*, San Antonio, Texas

Deering, R., and J. F. Kaiser, 2005, The Use of a Masking Signal to improve Empirical Mode Decomposition, *International Conference on Acoustics, Speech, and Signal Processing*, IEEE.

Feldman, M., 2011. Hilbert Transform Applications in Mechanical Vibration. Wiley.

Fosso, O., and M. Molinas, 2017, Method for Mode Mixing Separation in Empirical Mode Decomposition, IEEE.

Gonzalez, I., and R. Karoumi, 2014, Analysis of the annual variations in the dynamic behavior of ballasted railway bridge using Hilbert transform, Elsevier.

Rilling, G., and P. Flandrin, 2006, One or two Frequencies? The empirical Mode Decomposition Answers., *Signal Proc.*, IEEE.

Zeiler, A., 2012, Weighted Sliding Empirical Mode Decomposition and its Application to Neuromonitoring Data., Dissertation.